Pure Appl. Chem., Vol. 78, No. 1, pp. 15–27, 2006.
doi:10.1351/pac200678010015

Syntheses and applications of conducting polymer polyaniline nanofibers*

Jiaxing Huang‡

Department of Chemistry and Biochemistry and California NanoSystems Institute, University of California, Los Angeles, Los Angeles, CA 90095-1569, USA

Abstract: Nanofibers with diameters of tens of nanometers appear to be an intrinsic morphological unit that was found to "naturally" form in the early stage of the chemical oxidative polymerization of aniline. In conventional polymerization, nanofibers are subject to secondary growth of irregularly shaped particles, which leads to the final granular agglomerates. The key to producing pure nanofibers is to suppress secondary growth. Based on this, two methods—interfacial polymerization and rapidly mixed reactions—have been developed that can readily produce pure nanofibers by slightly modifying the conventional chemical synthesis of polyaniline without the need for any template or structural directing material. With this nanofiber morphology, the dispersibility and processibility of polyaniline are now much improved. The nanofibers show dramatically enhanced performance over conventional polyaniline applications such as in chemical sensors. They can also serve as a template to grow inorganic/polyaniline nanocomposites that lead to exciting properties such as electrical bistability that can be used for nonvolatile memory devices. Additionally, a novel flash welding technique for the nanofibers has been developed that can be used to make asymmetric polymer membranes, form patterned nanofiber films, and create polymer-based nanocomposites based on an enhanced photothermal effect observed in these highly conjugated polymeric nanofibers.

Keywords: conducting polymers; welding; memory device; nanocomposites; sensors; polyaniline; nanofibers.

INTRODUCTION

A tremendous amount of research has been carried out in the field of conducting polymers since 1977 when the conjugated polymer polyacetylene was discovered to conduct electricity through halogen doping [1–3]. The 2000 Nobel Prize in Chemistry recognized the discovery of conducting polymers and over 25 years of progress in this field [4,5]. In recent years, there has been growing interest in research on conducting polymer nanostructures (i.e., nano-rods, -tubes, -wires, and -fibers) since they combine the advantages of organic conductors with low-dimensional systems and therefore create interesting physicochemical properties and potentially useful applications [6–11]. Traditionally, an advantage of polymeric materials is that they can be synthesized and processed on a large scale at relatively low cost. And many of the applications (sensors, functional coatings, catalysts, etc.) of conducting polymers indeed need bulk quantity materials. Therefore, developing bulk syntheses for conducting polymers

Pure Appl. Chem.* **78, 1–64 (2006). A collection of invited, peer-reviewed articles by the winners of the 2005 IUPAC Prize for Young Chemists.
‡Current address: Department of Chemistry and Miller Institute for Basic Research in Science, University of California, Berkeley, Berkeley, CA 94720-1460, USA; Tel.: (510)-642-2867; Fax: (510)-642-7301; E-mail: jxhuang@berkeley.edu

would be especially important for practical reasons. This would enable an immediate evaluation of what nanostructures can bring to the properties and applications of conducting polymers.

In this brief review, polyaniline is used as a model material to systematically investigate the syntheses, properties, and applications of nanofibers of conjugated polymers. To begin, a conceptually new synthetic methodology is developed that readily produces high-quality, small-diameter nanofibers in large quantities. Next, the impact of this nanofibrillar morphology on the properties and applications of polyaniline is discussed. For example, it has been found that the nanofibers significantly improve the processibility of polyaniline and its performance in many conventional applications involving polymer interactions with its environment. This leads to much faster and more responsive chemical sensors, new inorganic/polyaniline nanocomposites, and ultra-fast nonvolatile memory devices. Additionally, the highly conjugated polymeric structure of polyaniline produces new nanoscale phenomena that are not accessible with current inorganic systems. As an example, the discovery of an enhanced photothermal effect that produces welding of the polyaniline nanofibers, is presented.

POLYANILINE NANOFIBERS: SYNTHESES AND FORMATION MECHANISM

Among the family of conjugated polymers, polyaniline is one of the most useful since it is air- and moisture-stable in both its doped, conducting form and in its de-doped, insulating form [12–14]. Polyaniline is also unique among conducting polymers in that it has a very simple acid/base doping/de-doping chemistry (Fig. 1). It has a great variety of potential applications including anticorrosion coatings, batteries, sensors, separation membranes, and antistatic coatings [2,3]. Conventional polyaniline synthesis (Figs. 1a,1b) is known to produce particulate products with irregular shapes. Therefore, many methods have been developed to make nanostructures of polyaniline (with diameters smaller than 100 nm) by introducing "structural directing agents" during the chemical polymerizing reaction. A great variety of such agents have been reported in the literature, and these include: surfactants [15–18], liquid crystals [19], polyelectrolytes [20], nanowire seeds [21], aniline oligmers [22], and relatively complex, bulky organic dopants [23–27]. It is believed that such functional molecules can either directly act as templates (e.g., polyelectrolytes) or promote the self-assembly of ordered "soft templates" (e.g., micelles, emulsions) that guide the formation of polyaniline nanostructures.

Intrinsic nanofibrillar morphology of polyaniline

It has been known from the early years of conducting polymer research that polyaniline fibrils of ~100 nm in diameter can form "naturally" during electrochemical polymerization on the surface of the electrodes [12,28,29]. Some recent work indicates that uniform polyaniline nanofibers can be obtained without the need for any template simply by controlling the electrochemical polymerization kinetics [30–32]. We have discovered that the basic morphological unit for chemically synthesized polyaniline also appears to be nanofibers with diameters of tens of nanometers [33], similar to those observed in polyacetylene [34]. First, through careful electron microscopy observations, a small amount of nanofibers can be found (Fig. 1c) among the irregularly shaped particulates in conventionally synthesized polyaniline [35,36]. This suggests the possibility of obtaining polyaniline nanofibers without any external structural directing agents. In a follow-up study, we periodically extracted the products during the polymerization reaction and examined the evolution of their morphology. A transition from pure, well-defined nanofibers, to irregularly shaped, micron-scale particulates was observed (Fig. 2). The overgrowth of polyaniline on the initially formed nanofiber scaffolds seems to be responsible for the formation of the final agglomerates in the product [33].

The nanofibers that formed naturally in the early stage of the polymerization reaction are smaller in diameter than most of the templated or electrospun fibers [37]. Therefore, in contrast to previous work in which preparation conditions were designed to "shape" the polymer into nanostructures, one can take advantage of the nanofibrillar morphological unit and focus on modifying the reaction path-

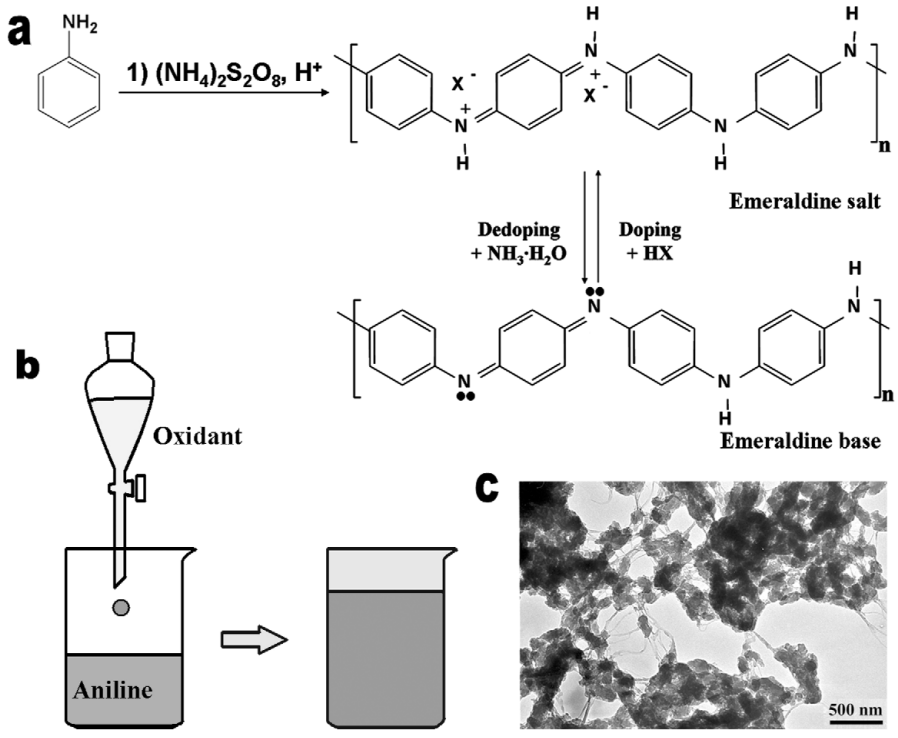

Fig. 1 The conventional synthesis of polyaniline and its morphology. (a,b) The oxidative polymerization reaction of aniline is typically carried out in an acidic solution (e.g., 1 M HCl). The as-prepared polyaniline is in its doped emeraldine form, which can be dedoped by a base to its emeraldine base form. (c) The typical morphology of the as-prepared polyaniline is irregularly shaped particles with a small amount of nanofibers.

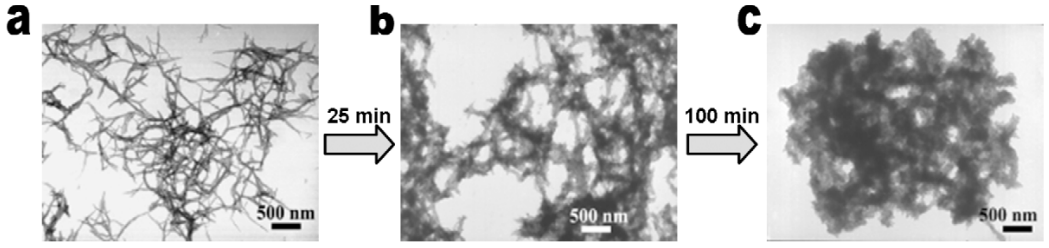

Fig. 2 Morphological evolution of polyaniline during its chemical polymerization in 1 M HCl. The transmission electron microscopy (TEM) images clearly show that (a) nanofibers are produced in the early stages of polymerization and then (b,c) turn into large, irregularly shaped agglomerates due to secondary growth. (Adapted from ref. [33]).

way so that nanofiber formation is favored while their overgrowth, which would otherwise lead to irregularly shaped agglomerates, is suppressed.

Making pure nanofibers: Suppressing secondary growth

Two basic approaches to separate nanofiber formation from overgrowth in conventional aniline polymerization reactions have been discovered. In the first approach, the reaction is placed in a heterogeneous biphasic system, where the polymerization occurs primarily at the interface (Fig. 3) [35,38].

Since the as-made polyaniline product is synthesized in its hydrophilic emeraldine salt form, it diffuses away from the reactive interface into the water layer. This makes more reaction sites available at the interface and avoids further overgrowth. In this way, the nanofibers formed at the interface are collected in the water layer without severe secondary overgrowth. Another method to prevent overgrowth is to stop the polymerization as soon as the nanofibers form. This has now been achieved by rapidly mixing the monomer and initiator solutions (Fig. 4) [33]. When the reaction starts, the initiator molecules are consumed rapidly during polymerization and depleted after nanofiber formation. Therefore, the overgrowth of polyaniline is suppressed due to lack of initiator molecules. The same synthetic approach has been successfully applied to polyaniline derivatives. For example, pure fibrillar poly(*m*-toluidine) (Fig. 5a), poly(*m*-fluoroaniline) (Fig. 5b), and poly(*m*-ethylaniline) (Fig. 5c) have been made from rapidly mixed reactions [39].

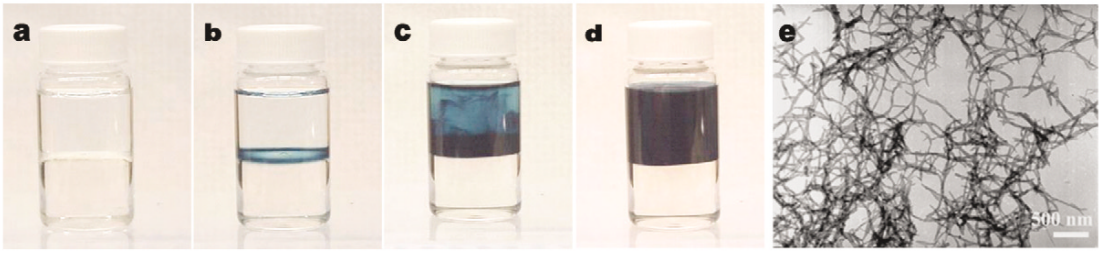

Fig. 3 Pure polyaniline nanofibers can be made by interfacial polymerization. In a typical reaction, (a) an aqueous solution of acid (1 M HCl) and oxidant and an organic solution of aniline are brought together to form an interface. (b) Polyaniline first forms at the interface and then (c,d) diffuses into the water layer since as-prepared polyaniline is in its hydrophilic emeraldine salt form. (e) The product is pure nanofibers as shown in the TEM image. (Adapted from ref. [48]).

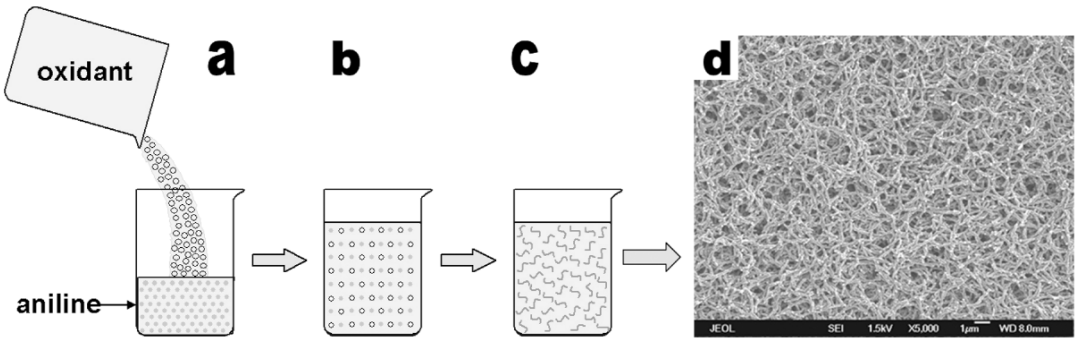

Fig. 4 Pure polyaniline nanofibers can also be made by rapidly mixed reactions. In a typical reaction, (a) the initiator and monomer solutions in 1 M HCl are rapidly mixed together all at once. Therefore (b,c) the initiator molecules are depleted during the formation of nanofibers, disabling further polymerization leading to overgrowth. (d) A typical scanning electron microscopy (SEM) image of nanofibers prepared in this manner. (Adapted from ref. [33]).

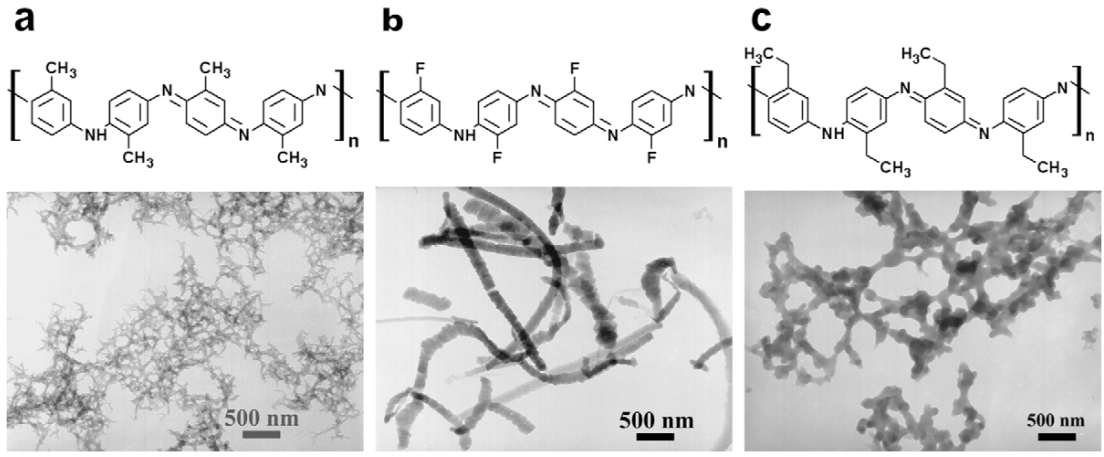

Fig. 5 Nanofibrillar structures are obtained for selective polyaniline derivatives using rapidly mixed reactions in 1 M HCl. (a) poly(*m*-toluidine), (b) poly(*m*-fluoroaniline), and (c) poly(*m*-ethylaniline).

Enhanced processibility of polyaniline nanofibers

The solution processibility and film-forming capability are of critical importance for the applications of a polymer. Polyaniline is insoluble in water, and it has been known to have poor water processibility, likely due to the irregularly shaped micron-sized morphology. Therefore, an adduct such as a water soluble polymer [e.g., poly(*N*-vinylpyrrolidone), PVP] is needed to form a polyaniline colloidal dispersion (see a recent IUPAC Technical Report in ref. [40]). However, polyaniline synthesized by either interfacial polymerization or rapidly mixed reactions exhibit excellent water dispersibility due to its uniform nanofibrillar morphology. For example, when purified by dialysis or centrifugation, polyaniline nanofibers readily disperse in water without any adduct. Casting such a dispersion onto a substrate, a mat of a random nanofiber network is obtained. Most interestingly, when the pH value of the solution is around 2.6, the nanofibers can form a stable colloidal dispersion by themselves [41]. This makes it very convenient to make nanofiber monolayer networks on negatively charged substrates such as glass due to the electrostatic interactions.

The synthetic methodology to polyaniline nanofibers presented here is conceptually different from previous work and is much simpler and more effective. Now high-quality polyaniline nanofibers can be readily made in large quantities in essentially any chemical laboratory [42–47,52]. The ease of synthesizing nanofibers and their water processibility should pave the way to many exciting discoveries and applications such as those described in the following sections. It should also provide important insights into the synthesis of other polymeric materials and even inorganic nanostructures.

POLYANILINE NANOFIBER-BASED CHEMICAL VAPOR SENSORS

Improved sensitivity and time response

Polyaniline is a promising material for sensors [48] since its conductivity is highly sensitive to chemical vapors. A common device platform for constructing such sensors is a chemiresistor (Fig. 6a, see page 23). In a typical polyaniline chemiresistor, a thin film of polyaniline is coated (usually by spin coating or drop casting) on electrodes as the sensitive layer for chemical vapors. On exposure to chemical vapors, a change in the film resistance can be readily recorded by a computer-controlled circuit. As can be seen from Fig. 6a (see page 23), the performance of such chemiresistors is determined by the interactions between vapor molecules and polymer. Poor diffusion of the vapor molecules can readily outweigh any improvements made to the polymer chains since most of the material other than the limited

number of surface sites is unavailable for interacting with the vapor, thus degrading sensitivity (Fig. 6c, see page 23). An immediate advantage of using nanofibers of polyaniline is that they shrink the diffusional path length for vapor molecules from the thickness of the film to the diameter of the nanofibers. For example, improvements in both sensitivity and time response of many orders of magnitude are now observed using the nanofibers (Figs. 6b,6c, see page 23) [38,49]. A great variety of chemical vapors including hydrochloric acid, ammonia, organic amines, hydrazine, chloroform, methanol, hydrogen sulfide, etc. have been tested and categorized. Five different mechanisms have been elucidated [50]. For each mechanistic type, significantly enhanced performance of nanofiber films over conventional materials is observed. The three-dimensional open structure of the nanofiber films also leads to some novel sensing properties. For example, for conventional film sensors, the response is strongly affected by the film thickness, however, the response of the porous nanofiber films is essentially thickness-independent (Fig. 6d, see page 23) [38,49].

Designing new reactions between polyaniline and chemical vapors

In order to detect a chemical vapor, the vapor–polyaniline interaction must produce a detectable change in the electrical conductivity of the film. Some acidic vapors such as H_2S are weak acids and therefore not strong enough to dope polyaniline, as can be seen from Figs. 7a and 7c (see page 23). This problem can be solved by converting the hard-to-detect H_2S into easily detected species upon interacting with polyaniline [51]. Note that H_2S can react rapidly with many metal salts (i.e., $CuCl_2$) to form a metal sulfide (i.e., CuS) and generate a strong acid as the by-product. Therefore, a new detecting mechanism for H_2S using metal salt modified polyaniline nanofibers has been designed (Fig. 7b, see page 23). Owing to their good water processibility, polyaniline nanofibers can be uniformly covered with a metal salt (e.g., $CuCl_2$) in an aqueous solution. The modified nanofibers show orders-of-magnitude enhancement in sensitivity on exposure to H_2S vapor (Fig. 7c, see page 23). This idea could be applicable to enhance the sensitivity for detecting many other weak acid vapors as well.

Polyaniline nanofiber chemical vapor sensor laboratory

Owing to the ease of the synthetic methods we have developed, sufficient nanofiber material is now readily available for chemical sensor applications. This should make polyaniline nanofibers a model material for sensor research as well as chemical/materials education. It is worth mentioning that a polyaniline nanofiber sensor laboratory has been incorporated into a Materials Creation Training Program laboratory class given in the UCLA Department of Chemistry and Biochemistry [52]. Students with no previous background in polymers or sensors learn the synthesis of polyaniline nanofibers, the construction of a simple sensing system, and the rapid detection of chemical vapors through a three-day laboratory assignment.

METAL-POLYANILINE NANOFIBER-BASED NANOCOMPOSITES AND DEVICES

Owing to the redox active nature of polyaniline, metal nanoparticles can be deposited on polyaniline nanofibers through a direct reaction between polyaniline nanofibers and oxidizing metal ions such as Au^{3+} and Ag^{+} [53]. The nanofibers can serve as a template to guide the growth of metal nanoparticles and/or confine them in the polymer matrix. The uniform diameters of the nanofibers lead to relatively narrow size distributions of the metal nanoparticles. For example, treating dedoped polyaniline nanofibers with a 10 mM $AgNO_3$ solution at room temperature (~25 °C) readily yields Ag nanoparticle decorated nanofibers in a dot-ON-fiber fashion (Fig. 8b). When the same reaction was refluxed in water at ~100 °C, three morphologies—dot-ON-fiber, dot-IN-fiber, and silver shells on nanofibers—were obtained (Figs. 8c,8d). This can be explained by understanding the diffusion and chemical processes occurring during the reaction (Fig. 8a). At reflux temperature, the rates of both the reduction

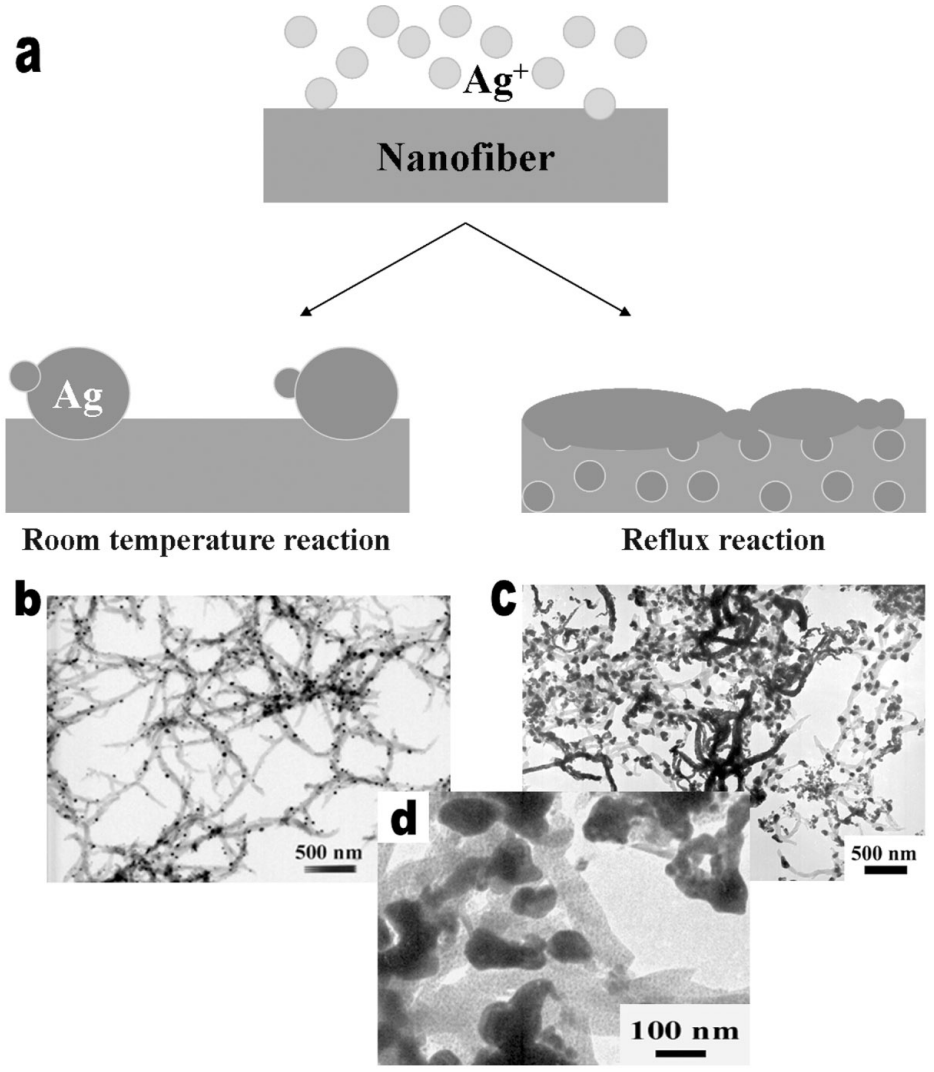

Fig. 8 Polyaniline nanofibers can guide the deposition of metal nanoparticles. (a) Schematic illustration showing two types of Ag-polyaniline composites obtained at ~25 °C and under reflux conditions (~100 °C, in water), respectively. (b) At room temperature, Ag nanoparticles (20–30 nm) are deposited on the nanofibers. (c,d) At boiling temperature, continuous Ag coating outside the nanofibers as well as small Ag nanoparticles (<10 nm) inside the nanofibers are both observed, likely due to enhanced ion reduction and diffusion rates, respectively.

reaction with polyaniline and the diffusion of Ag^+ into the nanofibers are enhanced, hence some Ag^+ may be forced into the nanofibers before the reaction is complete. Therefore, both dot-ON-fiber and dot-IN-fiber structures are obtained. The Ag nanoparticles outside the nanofiber can merge into neighboring particles and form a continuous shell on the nanofiber due to Ostwald ripening [54]. Under properly designed reaction conditions, it should be possible to have either the diffusion or the reaction overwhelm the other, leading to pure dot-ON-fiber or dot-IN-fiber types of Ag-polyaniline composites. Such composites should be promising materials for biosensing, catalysis, and nanoelectronics.

We have obtained pure dot-ON-fiber and dot-IN-fiber types of Au-polyaniline nanocomposites, respectively. As shown in Fig. 9, an interesting electrical bistability (Fig. 9d) has been discovered for

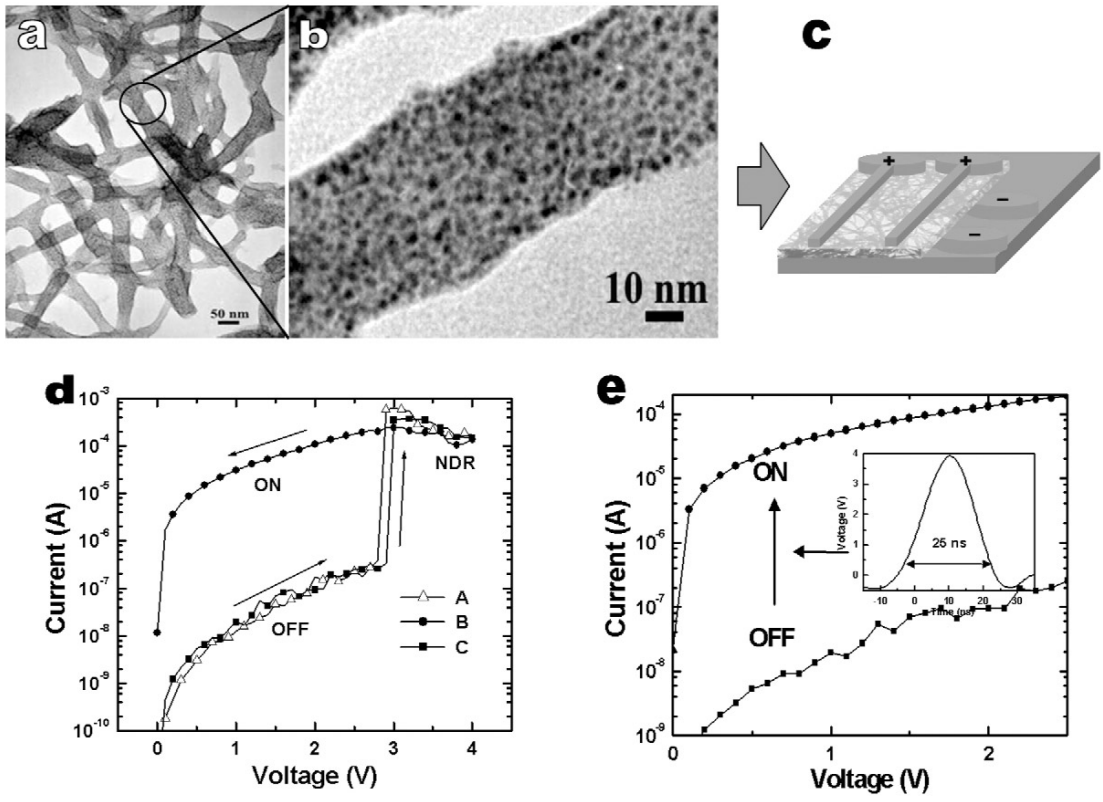

Fig. 9 Au-polyaniline nanocomposite (a,b) is a promising material for making ultra-fast nonvolatile memory devices (c). (c) A schematic illustration showing the sandwich type of device structure. (d) I-V characteristics of the polyaniline nanofiber/Au nanoparticle device. The potential is scanned from (A) 0 to +4 V, (B) +4 to 0 V, and (C) 0 to +4 V. (e) I-V characteristics of the OFF and the ON states of the device before and after the application of a voltage pulse of 4 V with a width of 25 ns, as shown in the inset. (Adapted from ref. [54]).

the dot-IN-fiber type of nanocomposite (Figs. 9a,9b) [55]. When the potential across the sandwich-type device (Fig. 9c) is increased to +3 V, an abrupt increase in current is observed. This changes the device from a low-conductivity OFF state to a high-conductivity ON state (Fig. 9d, curve A). The device is stable in the ON state when the potential is lowered back to 0 V (Fig. 9d, curve B). The high conductivity of the ON state can be changed back to the OFF state by applying a reverse bias of –5 V. The device is then stable in the OFF state until +3 V is applied, at which point it returns to the ON state (Fig. 9d, curve C). This electrical bistability can be used to construct polyaniline-based nonvolatile memory devices (PANI-MEM). Such devices are found to have nanosecond switching times (Fig. 9e), high on/off ratios, and potentially low manufacturing costs, making them promising for faster and less expensive nonvolatile data storage media than what is currently available (e.g., flash memory).

FLASH WELDING OF CONDUCTING POLYMER NANOFIBERS

While the nanoscale structure of polyaniline nanofibers produces enhanced polymer functionalities, their polymeric nature also yields new nanoscale physicochemical phenomena that have not been observed in inorganic nanostructured materials. As an example, a flash welding technique is presented based on an enhanced photothermal effect discovered with the polyaniline nanofibers (Fig. 10) [56].

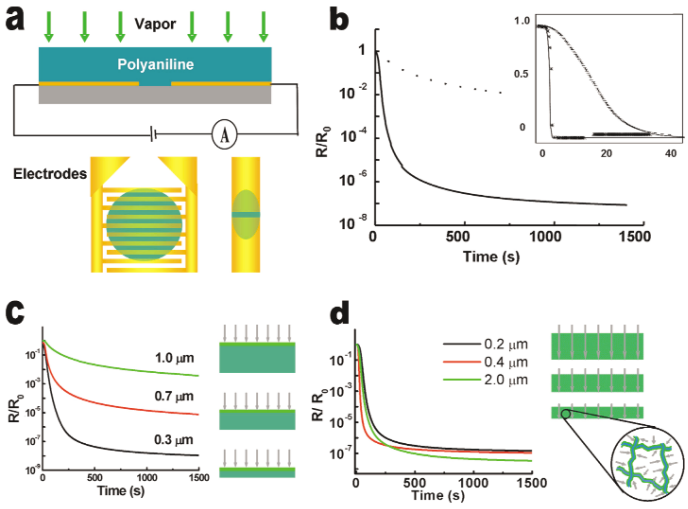

Fig. 6 The fibrillar nanostructure significantly improves polyaniline's performance in chemical vapor sensor applications. (a) Schematic illustration showing a polyaniline chemiresistor sensor, a set of polyaniline-coated interdigitated electrodes and a pair of simple gap electrodes. (b) On exposure to 100 ppm of HCl vapor (solid line), the response of the nanofiber film is 6 orders of magnitude higher than that of (dotted line) a conventional polyaniline film. The time response of the nanofiber film is ~2 s, while that of the conventional film is ~40 s (see inset of b). (c) The sensitivity of conventional thin film sensors is strongly affected by their thickness, while (d) that of the nanofiber films is essentially independent of the thickness. (b is adapted from ref. [49]; c,d are adapted from ref. [48]).

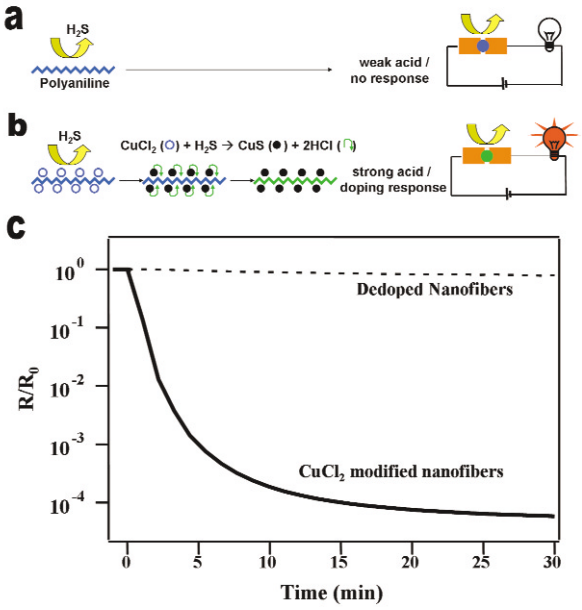

Fig. 7 New sensing mechanisms can be designed based on the new properties of nanofibrillar polyaniline, expanding its capability for detection. For example, (a) polyaniline nanofibers are not sensitive to H_2S gas (c, dotted line) since it is too weak an acid to be a dopant for polyaniline. However, due to their good water dispersibility (b), polyaniline nanofibers can be uniformly modified by an aqueous solution of metal salt (e.g., $CuCl_2$), leading to orders-of-magnitude enhancement in sensitivity (c, solid line) due to doping by in situ generated HCl.

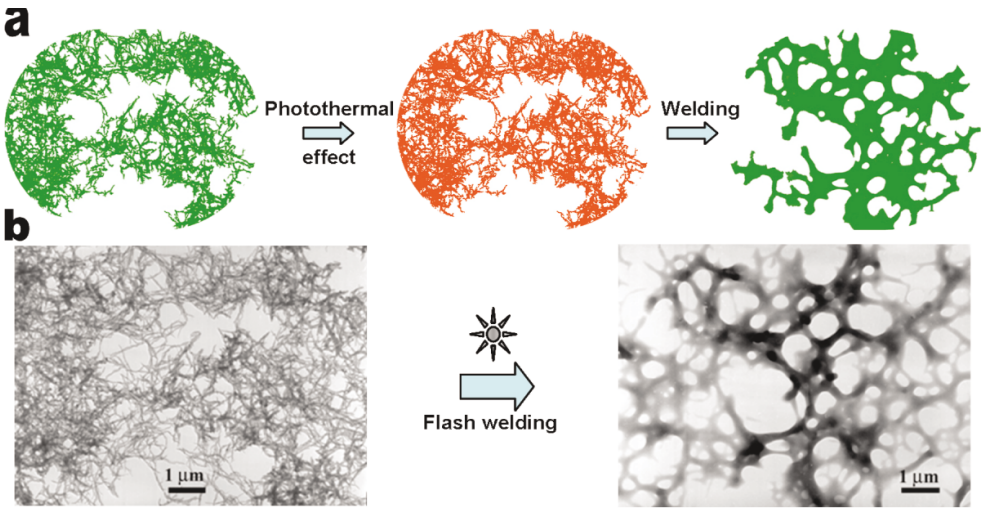

Fig. 10 Polyaniline nanofibers can be welded together (b) on exposure to a camera flash due to locally confined heat produced by an enhanced photothermal effect (a). (Adapted from ref. [55]).

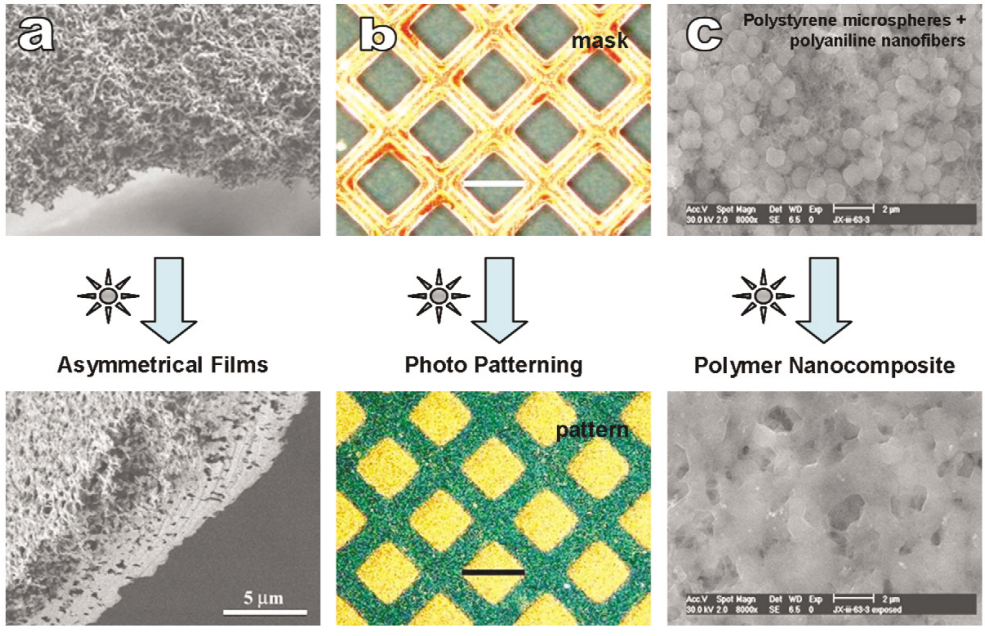

Fig. 11 Potential applications of the flash welding technique: (a) Making asymmetric polymer membranes. The top SEM image shows a polyaniline nanofiber film deposited on a Si substrate. The cross-section of a nanofiber film after exposure to a camera flash is shown in the bottom SEM image. The density difference before (the front, unexposed side) and after (the back, exposed side) flash welding can be clearly seen. (b) Creating patterns in nanofiber films. The top optical microscopy image shows a copper grid mask lying on top of a polyaniline nanofiber film. After exposure to a camera flash, the grid pattern is generated on the nanofiber film. The unmasked diamond shaped areas are welded, therefore, reflect more light and look bright under an optical microscope. The previously masked areas still look green (scale bar: 100 μm). (c) Producing polymer-polymer nanocomposites. For example, a blend of polystyrene spheres (diameter ~1 μm) and polyaniline nanofibers can be welded together by flash welding as shown in the SEM images. (Adapted from ref. [55]).

When polyaniline is exposed to light, it converts most of the absorbed energy into heat due to its high photothermal conversion efficiency [57–59]. In polyaniline nanofibers, the heat generated through photothermal processes will be confined within the individual nanofibers (Fig. 10a) since polyaniline, as well as other polymeric materials, is a poor heat conductor. This enables unprecedented photothermal effects that cannot be observed in either bulk polyaniline or inorganic nanomaterials [60–62]. A camera flash is found to cause instantaneous welding of conducting polymers. Under flash irradiation, polyaniline nanofibers instantly "melt" to form a smooth and continuous film from an originally random network of nanofibers (Fig. 10b). This flash welding technique can lead to many exciting potential applications (Fig. 11). For example, when a nanofiber film is flashed, only the exposed side is welded while the unexposed side remains intact. Therefore, a free-standing asymmetric membrane can be created directly from a nanofiber powder film (Fig. 11a). Since the welded film becomes smoother and reflects more light, flash welding can be used to imprint patterns into nanofiber films by using a photomask (Fig. 11b). Moreover, the heat generated during flash irradiation can also weld polyaniline to another polymer such as polystyrene (Fig. 11c) or even Teflon® (polytetrafluoroethylene). Flash welding thus enables a wide range of potential applications from forming asymmetric nanofiber films to rapidly melt-blending polymer-polymer nanocomposites to photo-patterning polymer nanofiber films. Flash welding should be a general phenomenon for nanomaterials with the following characteristics: high absorbance (i.e., deeply colored), high photothermal efficiency (i.e., low emission), low thermal conductivity, and a phase change before structural breakdown.

CONCLUSIONS

Examining the morphological evolution of polyaniline during its chemical polymerization reveals that it preferentially forms as nanofibers in aqueous solution. By preventing secondary growth, pure nanofibers can be obtained. Two facile approaches—interfacial polymerization and rapidly mixed reactions—have been developed that readily produce high-quality nanofibers. The impact of this pure nanofibrillar morphology on the properties of polyaniline, in general, lies in significantly improved interactions of polyaniline with its environment. This leads to the nanofibers' excellent water processibility, much faster and more responsive chemical sensors, new inorganic/polyaniline nanocomposites, and ultra-fast nonvolatile memory devices. On the other hand, flash welding of the highly conjugated, polymeric nanofibers demonstrates a new nanoscale phenomenon that is not accessible with current inorganic systems. The work presented in this short review clearly demonstrates the advantages of "nanostructures + conducting polymers". Conducting polymers thus have an important role to play in the emerging field of nanoscience.

ACKNOWLEDGMENTS

I would like to thank my graduate advisor, Prof. Richard Kaner, for introducing me to the fascinating field of conducting polymers, and his constant support during and beyond my graduate school years at UCLA. I also thank Dr. B. H. Weiller, S. Virji (The Aerospace Corporation), and Dr. R. G. Blair for collaborative work on chemical sensors and Prof. Y. Yang and R. Tseng for collaborative work on memory devices. The financial and program support of the Microelectronics Advanced Research Corporation (MARCO) and its focus center on Functional Engineered NanoArchitectonics (FENA) is gratefully acknowledged.

REFERENCES

1. H. Shirakawa, E. J. Louis, A. G. MacDiarmid, C. K. Chiang, A. J. Heeger. *Chem. Commun.* 578 (1977).
2. T. J. Skotheim, R. L. Elsenbaumer, J. R. Reynolds. *Handbook of Conducting Polymers*, 2nd ed., p. 1097, Marcel Dekker, New York (1998).
3. P. Chandrasekhar. *Conducting Polymers, Fundamentals and Applications: A Practical Approach*, p. 760, Kluwer Academic, Boston (1999).
4. A. G. MacDiarmid. *Angew. Chem., Int. Ed.* **40**, 2581 (2001).
5. N. Hall. *Chem. Commun.* 1 (2003).
6. M. J. Sailor and C. L. Curtis. *Adv. Mater.* **6**, 688 (1994).
7. S. Neves, W. A. Gazotti, M.-A. De Paoli. In *Encyclopedia of Nanoscience and Nanotechnology*, Vol. 2, H. S. Nalwa (Ed.), pp. 133–152, American Scientific Publishers, Los Angeles (2004).
8. R. Gangopadhyay. In *Encyclopedia of Nanoscience and Nanotechnology*, Vol. 2, H. S. Nalwa (Ed.), pp. 105–131, American Scientific Publishers, Los Angeles (2004).
9. G. G. Wallace, P. C. Innis, L. A. P. Kane-Maguire. In *Encyclopedia of Nanoscience and Nanotechnology*, Vol. 4, H. S. Nalwa (Ed.), pp. 113–130, American Scientific Publishers, Los Angeles (2004).
10. A. J. Epstein. In *Organic Electronic Materials: Conjugated Polymers and Low Molecular Weight Organic Solids*, Vol. 41, R. Farchioni and G. Grosso (Eds.), p. 3, Springer, Amsterdam (2001).
11. C. R. Martin. *Acc. Chem. Res.* **28**, 61 (1995).
12. W. S. Huang, B. D. Humphrey, A. G. MacDiarmid. *J. Chem. Soc., Faraday Trans. 1* **82**, 2385 (1986).
13. A. G. MacDiarmid. *Synth. Met.* **84**, 27 (1997).
14. A. G. MacDiarmid, J. C. Chiang, M. Halpern, W. S. Huang, S. L. Mu, N. L. D. Somasiri, W. Q. Wu, S. I. Yaniger. *Mol. Cryst. Liq. Cryst.* **121**, 173 (1985).
15. X. Zhang and S. K. Manohar. *Chem. Commun.* **20**, 2360 (2004).
16. L. Yu, J. I. Lee, K. W. Shin, C. E. Park, R. Holze. *J. Appl. Polym. Sci.* **88**, 1550 (2003).
17. J. C. Michaelson and A. J. McEvoy. *Chem. Commun.* 79 (1994).
18. G. C. Li and Z. K. Zhang. *Macromolecules* **37**, 2683 (2004).
19. L. M. Huang, Z. B. Wang, H. T. Wang, X. L. Cheng, A. Mitra, Y. X. Yan. *J. Mater. Chem.* **12**, 388 (2002).
20. J. M. Liu and S. C. Yang. *Chem. Commun.* 1529 (1991).
21. X. Zhang, W. J. Goux, S. K. Manohar. *J. Am. Chem. Soc.* **126**, 4502 (2004).
22. W. G. Li and H. L. Wang. *J. Am. Chem. Soc.* **126**, 2278 (2004).
23. H. J. Qiu, M. X. Wan, B. Matthews, L. M. Dai. *Macromolecules* **34**, 675 (2001).
24. Z. X. Wei and M. X. Wan. *J. Appl. Polym. Sci.* **87**, 1297 (2003).
25. Z. X. Wei, Z. M. Zhang, M. X. Wan. *Langmuir* **18**, 917 (2002).
26. M. X. Wan. In *Encyclopedia of Nanoscience and Nanotechnology*, Vol. 2, H. S. Nalwa (Ed.), pp. 153–169, American Scientific Publishers, Los Angeles (2004).
27. H. J. Qiu and M. X. Wan. *J. Polym. Sci., Part A: Polym. Chem.* **39**, 3485 (2001).
28. J. G. Mantovani, R. J. Warmack, B. K. Annis, A. G. Macdiarmid, E. Scherr. *J. Appl. Polym. Sci.* **40**, 1693 (1990).
29. Y. Wei, Y. Sun, G.-W. Jang, X. Tang. *J. Polym. Sci., Part C: Polym. Lett.* **28**, 81 (1990).
30. S. J. Choi and S. M. Park. *J. Electrochem. Soc.* **149**, E26 (2002).
31. J. Liu, Y. H. Lin, L. Liang, J. A. Voigt, D. L. Huber, Z. R. Tian, E. Coker, B. Mckenzie, M. J. Mcdermott. *Chem. Eur. J.* **9**, 605 (2003).
32. L. Liang, J. Liu, C. F. Windisch, G. J. Exarhos, Y. H. Lin. *Angew. Chem., Int. Ed.* **41**, 3665 (2002).
33. J. X. Huang and R. B. Kaner. *Angew. Chem., Int. Ed.* **43**, 5817 (2004).

34. J. C. W. Chien, Y. Yamashita, J. A. Hirsch, J. L. Fan, M. A. Schen, F. E. Karasz. *Nature* **299**, 608 (1982).
35. J. X. Huang and R. B. Kaner. *J. Am. Chem. Soc.* **126**, 851 (2004).
36. D. Chao, J. Chen, X. Lu, L. Chen, W. Zhang, Y. Wei. *Synth. Met.* **150**, 47 (2005).
37. A. G. MacDiarmid, W. E. Jones, I. D. Norris, J. Gao, A. T. Johnson, N. J. Pinto, J. Hone, B. Han, F. K. Ko, H. Okuzaki, M. Llaguno. *Synth. Met.* **119**, 27 (2001).
38. J. X. Huang, S. Virji, B. H. Weiller, R. B. Kaner. *J. Am. Chem. Soc.* **125**, 314 (2003).
39. J. X. Huang and R. B. Kaner. *Chem. Commun.* (2006) DOI: 10.1039/b510956f.
40. J. Stejskal and I. Sapurina. *Pure Appl. Chem.* **77**, 815 (2005).
41. D. Li and R. B. Kaner. *Chem. Commun.* 3286 (2005).
42. P. L. B. Araujo, E. S. Araujo, R. F. S. Santos, A. P. L. Pacheco, *Microelectron. J.* **36**, 1055 (2005).
43. Y. He. *Mater. Sci. Eng., B* **122**, 76 (2005).
44. A. R. Hopkins, D. D. Sawall, R. M. Villahermosa, R. A. Lipeles. *Thin Solid Films* **469–470**, 304 (2004).
45. X. Zhang, R. Chan-Yu-King, A. Jose, S. K. Manohar. *Synth. Met.* **145**, 23 (2004).
46. J. Jang, J. Bae, K. Lee. *Polymer* **46**, 3677 (2005).
47. N.-R. Chiou and A. J. Epstein. *Adv. Mater.* **17**, 1679 (2005).
48. J. Janata and M. Josowicz. *Nat. Mater.* **2**, 19 (2003).
49. J. X. Huang, S. Virji, B. H. Weiller, R. B. Kaner. *Chem. Eur. J.* **10**, 1314 (2004).
50. S. Virji, J. X. Huang, R. B. Kaner, B. H. Weiller. *Nano Lett.* **4**, 491 (2004).
51. S. Virji, J. D. Fowler, C. O. Baker, J. X. Huang, R. B. Kaner, B. H. Weiller. *Small* **1**, 624 (2005).
52. E. K. Wilson. *Chem. Eng. News* **83**, 37 (2005).
53. J. G. Wang, K. G. Neoh, E. T. Kang. *J. Colloid Interface Sci.* **239**, 78 (2001).
54. W. Ostwald. *Z. Phys. Chem.* **22**, 289 (1897).
55. R. J. Tseng, J. X. Huang, J. Ouyang, R. B. Kaner, Y. Yang. *Nano Lett.* **5**, 1077 (2005).
56. J. X. Huang and R. B. Kaner. *Nat. Mater.* **3**, 783 (2004).
57. T. Toyoda and H. Nakamura. *Jpn. J. Appl. Phys., Part 1* **34**, 2907 (1995).
58. J. E. De Albuquerque, W. L. B. Melo, R. M. Faria. *J. Polym. Sci., Part B: Polym. Phys.* **38**, 1294 (2000).
59. J. E. De Albuquerque, W. L. B. Melo, R. M. Faria. *Rev. Sci. Instrum.* **74**, 306 (2003).
60. N. Braidy, G. A. Botton, A. Adronov. *Nano Lett.* **2**, 1277 (2002).
61. P. M. Ajayan, M. Terrones, A. de la Guardia, V. Huc, N. Grobert, B. Q. Wei, H. Lezec, G. Ramanath, T. W. Ebbesen. *Science* **296**, 705 (2002).
62. N. Wang, B. D. Yao, Y. F. Chan, X. Y. Zhang. *Nano Lett.* **3**, 475 (2003).